PHYSICS OF FLUIDS **25**, 110823 (2013)

Reynolds number scaling of coherent vortex simulation and stochastic coherent adaptive large eddy simulation

Alireza Nejadmalayeri,[a] Alexei Vezolainen,[b] and Oleg V. Vasilyev[c]
Department of Mechanical Engineering, University of Colorado Boulder, Boulder, Colorado 80309-0427, USA

(Received 16 December 2012; accepted 30 September 2013; published online 23 October 2013)

In view of the ongoing longtime pursuit of numerical approaches that can capture important flow physics of high Reynolds number flows with fewest degrees of freedom, two important wavelet-based multi-resolution schemes are thoroughly examined, namely, the Coherent Vortex Simulation (CVS) and the Stochastic Coherent Adaptive Large Eddy Simulation (SCALES) with constant and spatially/temporarily variable thresholding. Reynolds number scaling of active spatial modes for CVS and SCALES of linearly forced homogeneous turbulence at high Reynolds numbers is investigated in *dynamic* study for the first time. This *dynamic* computational complexity study demonstrates that wavelet-based methods can capture flow-physics while using substantially fewer degrees of freedom than both direct numerical simulation and marginally resolved LES with the same level of fidelity or turbulence resolution, defined as ratio of subgrid scale and the total dissipations. The study provides four important observations: (1) the linear Reynolds number scaling of energy containing structures at a fixed level of kinetic energy, (2) small, close to unity, fractal dimension for constant-threshold CVS and SCALES simulations, (3) constant, close to two, fractal dimension for constant-dissipation SCALES that is insensitive to the level of fidelity, and (4) faster than quadratic decay of the compression ratio as a function of turbulence resolution. The very promising slope for Reynolds number scaling of CVS and SCALES demonstrates the potential of the wavelet-based methodologies for hierarchical multiscale space/time adaptive variable fidelity simulations of high Reynolds number turbulent flows. © *2013 AIP Publishing LLC*. [http://dx.doi.org/10.1063/1.4825260]

I. INTRODUCTION

Direct Numerical Simulation (DNS),[1] despite four decades of its existence, still remains only a tool for turbulence research,[2] since for flows of engineering interest it is virtually impossible to resolve all the physically meaningful scales within the limit of continuum mechanics from integral length scale L (the characteristic length-scale of the physical domain) all the way down to the smallest dissipative Kolmogorov length scale η. This daunting range of spatial scales that increases with Reynolds number, $\frac{L}{\eta} \approx Re^{3/4}$, implies an enormous computational complexity for spatial modes that scales like $Re^{9/4}$ or $Re_\lambda^{9/2}$ in terms of Taylor microscale Reynolds number. Thus, total number of floating-point operations (considering both spatial and temporal modes) scales like Re^3. For instance, for typical aeronautical applications where Re is at least of the order of few millions, DNS requires more than 10^{18} number of operations making it impractical for real flow applications, at least until quantum computers become a reality.

[a]Electronic mail: alireza.nejadmalayeri@colorado.edu
[b]Electronic mail: alexei.vezolainen@colorado.edu
[c]Electronic mail: oleg.vasilyev@colorado.edu. URL: http://multiscalemodeling.colorado.edu.

This classical scaling is too pessimistic since the bound neglects spatial and temporal intermittency.[3] In reality, the turbulent flows are highly intermittent and active degrees of freedom (DOFs) extend over many "limited" number of scales. As a result, turbulent structures can be uniquely determined by a finite number of spatial modes at each time.[3–5] On the other hand, according to recent observations by Yakhot and Sreenivasan,[6] the strongest and rarest fluctuations could occur at scales smaller than Kolmogorov scale resulting in Re^4 instead of Re^3 scaling. However, once again, their investigation was performed on a uniform computational grid and they commented that the space-time DOFs could in fact be smaller than Re^3 if only the "interesting" parts of the flow were resolved.

Large Eddy Simulation (LES), despite its success in modeling flows of engineering interest, e.g., Refs. 7 and 8, does not address these challenges, mainly because the computational affordability is achieved by modeling the effect of high wavenumbers and not resolving the small-scale physics. On the other hand, marginally resolved LES, where the ratio of subgrid scale (SGS) and resolved dissipations is relatively small, scales similar to DNS, $Re_\lambda^{9/2}$, mainly because the requirement of resolving most of the dissipation results in the filter width close to the actual peak of energy dissipation. Thus, the only feasible alternative in the quest for methodologies that capture interesting/important physics of high Reynolds number turbulent flows is the use of adaptive numerical approaches that can extract only the essential DOFs in order to make such simulations feasible for practical engineering purposes. Wavelet-based multi-resolution variable fidelity methodologies for simulations of turbulence[9] are great candidates for resolving highly intermittent turbulent flows, decomposing turbulent flow into deterministic coherent and stochastic incoherent structures, and extracting energetic structures.

The most notable wavelet-based methodologies for computational simulations of turbulent flows are Coherent Vortex Simulation (CVS) and Stochastic Coherent Adaptive Large Eddy Simulation (SCALES). Both techniques use the wavelet-thresholding filter to solve the vorticity transport or Navier-Stokes equations, respectively. In brief, CVS[10] is a technique to decompose the flow into deterministic coherent and stochastic incoherent modes while SCALES[11] resolves the most-energetic deterministic coherent structures and models the effect of less-energetic coherent/incoherent modes. The compression accomplished by wavelets has been extensively studied for both CVS[12,13] and SCALES.[11] The first attempt to systematically study how compression rate of 3D homogeneous turbulence depends on the Reynolds number was given in Ref. 12, where it was shown in *a priori* study of spectral DNS data that the number of coherent modes of homogenous turbulence scales like $Re_\lambda^{3.9}$.

Many factors such as adaptive computational mesh, the truncation error of wavelet polynomial approximation, aliasing, the adjacent (safety) zone used in the adaptive wavelet-based algorithms, the numerical dissipation induced by the wavelet truncation, as well as physical model (including no model for CVS or perfect SGS model[14] for SCALES) can alter the energy and enstrophy cascades in true simulations and change the number of degrees of freedom compared to *a priori* CVS[12] and SCALES[11] studies. Thus, in order to fully assess the computational complexity of the actual CVS and SCALES, one needs to perform *dynamic* studies. The present work is the first systematic *dynamic* study that provides a quantitative description of Reynolds number scaling of the number of active spatial modes used in actual CVS and SCALES simulations of three dimensional homogeneous turbulence.

It should be emphasized that in addition to the wavelet compression, known as the most prominent strength of wavelets in turbulence, the ability of wavelet-based methodologies to actively control the level of capturing/modeling of the desired flow-physics is even more unique. The specified level of fidelity or turbulence resolution, defined as a ratio of SGS and total dissipations, can be controlled by means of a recently developed continuously variable fidelity space/time/model-form adaptive methodology[15] capable of dynamic adaptation of computational mesh and model-fidelity to ensure the spatially and temporarily uniform turbulence resolution. The two-way coupling between numerical resolution and physical models is achieved through the use of spatio-temporal variation of the wavelet thresholding factor, which controls both the local numerical resolution and modeled dissipation. This variable fidelity approach provides a unique framework for performing a *dynamic* computational complexity study of SCALES, where the Reynolds number scaling for different levels of turbulent resolution can be explored. It should be noted that due to two-way coupling of

the physical model and numerics, the variable fidelity computational complexity studies can only be performed *in silico* using actual simulations. Therefore, this work does not only present the Reynolds number scaling of CVS and SCALES, but also demonstrates how wavelet-based turbulence modeling methodologies resolve more flow-physics using profoundly smaller number of spatial modes with the efficiency that improves with the increase of Reynolds number.

II. WAVELET THRESHOLDING FILTER

In the wavelet-based approach to the numerical simulation of turbulence, the separation between resolved energetic structures and unresolved residual flow is obtained through nonlinear multi-resolution wavelet threshold filtering (WTF). The filtering procedure is accomplished by applying the wavelet-transform to the unfiltered velocity field, discarding the wavelet coefficients below a given threshold (ϵ) and transforming back to the physical space. This results in decomposition of the turbulent velocity field into two different parts: a more energetic velocity field and a residual less energetic one, i.e., $u_i = \overline{u}_i^{>\epsilon} + u_i'$, where $\overline{u}_i^{>\epsilon}$ stands for the wavelet-filtered velocity at level ϵ

$$\overline{u}_i^{>\epsilon}(\mathbf{x}) = \sum_{\mathbf{l}\in\mathcal{L}^1} c_{\mathbf{l}}^1 \phi_{\mathbf{l}}^1(\mathbf{x}) + \sum_{j=1}^{+\infty}\sum_{\mu=1}^{2^n-1} \sum_{\substack{\mathbf{k}\in\mathcal{K}^{\mu,j} \\ |d_{\mathbf{k}}^{\mu,j}|>\epsilon\|u_i\|_{\mathrm{WTF}}}} d_{\mathbf{k}}^{\mu,j}\psi_{\mathbf{k}}^{\mu,j}(\mathbf{x}), \tag{1}$$

where $\psi_{\mathbf{k}}^{\mu,j}$ are wavelets of family μ at j level of resolution, $d_{\mathbf{k}}^{\mu,j}$ are the coefficients of the wavelet decomposition, and $\phi_{\mathbf{l}}^1$ are scaling functions at the coarsest level of resolution. In this decomposition, bold subscripts denote an index in n-dimensional space, e.g., $\mathbf{k} = (k_1, \ldots, k_n)$, while $\mathcal{L}^1$ and $\mathcal{K}^{\mu,j}$ are n-dimensional index sets associated with scaling functions at the first (coarsest) level of resolution ($\phi_{\mathbf{l}}^1$) and wavelets of family μ and level j ($\psi_{\mathbf{k}}^{\mu,j}$), respectively. More details of the wavelet thresholding filter can be found, for instance, in Ref. 16 and the details about the type and shape of the wavelets employed in the current approach can be found in Ref. 11.

The key-role in the wavelet-filter definition is clearly played by the non-dimensional relative thresholding level ϵ that explicitly defines the relative energy level of the eddies that are resolved and, consequently, controls the importance of the influence of the residual field on the dynamics of the resolved motions.

III. ADAPTIVE WAVELET COLLOCATION METHOD

In the current work, the parallel[15] version of the Adaptive Wavelet Collocation Method (AWCM)[17–20] based on the "second generation wavelets"[21] is used. In AWCM, the partial differential equations (PDEs) are solved in physical space on an adaptive nested (dyadic) computational grid. This prevents the major difficulties associated with adaptive wavelet Galerkin methods: challenging treatment of nonlinearities and general boundary conditions. The evaluation of the nonlinear terms in adaptive wavelet collocation methods is performed in the physical domain similar to pseudo-spectral methods. The grid adaptation in wavelet collocation methods is done similar to other wavelet-based methods. That is to say, the grid adaption strategy is based on analyzing the wavelet coefficients $d_{\mathbf{k}}^{\mu,j}$.

The wavelet thresholding criterion is adequate for representing a function or a field with fewest degrees of freedom, while actively controlling the accuracy of the approximation. However, for solving PDEs, it is imperative to ensure that the wavelet basis or computational mesh is sufficient to approximate the solution throughout the time-integration step for the evolution problems or at the next iteration in the elliptic problems. In order to ensure the adequate approximation of the solution during time integration, the concept of a safety or an adjacent zone is introduced, which includes wavelets whose coefficients are or can possibly become significant during the period of time integration, when the grid remains unchanged. This safety zone includes neighboring wavelets at the same, above (children), and below (ancestors) levels of resolution at each significant point. Once the approximation (1) is constructed, the computational grid is obtained based on

one-to-one correspondence between wavelets and collocation points: a collocation point is kept if the corresponding wavelet is kept in the approximation (1).

The AWCM has been developed and thoroughly investigated for parabolic,[17,18] hyperbolic,[22] and elliptic[19] partial differential equations. It was successfully applied to a wide spectrum of compressible and incompressible flows including fluid-structure interaction,[20] wavelet-based adaptive large eddy simulation,[11,23,24] Rayleigh-Taylor instability,[25] ocean modeling,[26] and combustion.[27]

IV. WAVELET-BASED TURBULENCE MODELING METHODS

Wavelet-based turbulence modeling techniques are primarily classified as Wavelet-based DNS (WDNS), CVS, and SCALES. WDNS[28] solves the wavelet-filtered Navier-Stokes equations using a wavelet-based numerical method without any model with a sufficiently small threshold in order to ensure that the ignored modes are insignificant. WDNS can be viewed as adaptive-DNS, which as a result of compression of wavelet filtering retains a smaller number of spatial modes compared with DNS; however, still due to small threshold, it is extremely expensive and not a practical tool for high Reynolds number flow applications.

In CVS[10] the vorticity is decomposed by wavelet filter (1) with an ideal threshold-value ϵ_{ideal} into deterministic coherent and stochastic incoherent structures. The coherent structures are mostly responsible for the evolution of the turbulence and turbulent energy cascade, while the effect of background incoherent modes can be neglected because of its Gaussian white-noise PDF. CVS achieves a significant compression compared with DNS; however, number of remaining active modes are still large and the process of calculating the ideal threshold at each time-step is quite expensive since it requires the variance of the incoherent modes. Moreover, the wavelet-based coherent vortex extraction for inhomogeneous turbulence is still an open question.[9]

Hence, the idea of SCALES,[11] which inherits the advantages of both CVS and LES while overcoming the shortcomings of both, was proposed based on the notion of filtering the velocity field using wavelet-thresholding filter with threshold-level of higher than the ideal threshold-value used in CVS. In SCALES the flow is decomposed into more and less energetic structures and as a result the effect of background flow cannot be ignored and needs to be modeled similar to LES. The wavelet-threshold filtering at a higher threshold-level as well as the use of SGS models to take the effect of filtered-out modes result in a smaller number of degrees-of-freedom than CVS and consequently a higher grid-compression can be achieved. Furthermore, the filtering and consequently, the SGS models are benefited from wavelet nonlinear multiscale band-pass filter, which depends on instantaneous flow realization. In other words, one can view SCALES as an adaptive large eddy simulation that, unlike classical LES, takes advantage of turbulence intermittency by dynamically adjusting the filter width both in space and time.

All in all, CVS and LES are limiting cases of coherent/incoherent and large/small structures distinctions, while in SCALES the separation is more relaxed. Therefore, while CVS is computationally expensive for high Reynolds number turbulent flows, majority of important energetic structures are resolved and both coherent-deterministic and incoherent-stochastic unresolved modes can be modeled. This distinction is not anymore limited to the size of the structures, as it is the case of classical LES. Furthermore, resolved structures and the modeled eddies overlap over a range of wavenumbers together in order to ensure more realistic energy cascade.

It should be mentioned that CVS in its original formulation[10] solves the wavelet-filtered vorticity equations with the use of orthogonal Daubechies wavelets, while SCALES analogous to LES solves wavelet-filtered Navier-Stokes equations along with SGS models using bi-orthogonal second generation interpolated wavelets. However, Goldstein and Vasilyev[11] showed that the velocity-field can be decomposed into deterministic coherent and stochastic incoherent (with Gaussian PDF) modes using wavelet threshold filtering in velocity space, thus, CVS can also be based on primitive variables (velocity-pressure). Therefore, hereafter we refer to CVS in velocity-pressure formulation. This implies that this CVS and SCALES both solve the wavelet-threshold filtered Navier-Stokes equations without and with SGS models, respectively, though at different threshold levels. Hence, in both CVS and SCALES, the wavelet-filtered Navier-Stokes equations are solved using the adaptive wavelet collocation method discussed in Sec. III. Unlike the original CVS where the ideal threshold

can be calculated based on the variance of the incoherent modes, in this velocity-based CVS, the optimal threshold should be found by numerical experiment.

V. REYNOLDS NUMBER SCALING CASE STUDY

To construct the Reynolds number scaling statistics, a series of CVS and SCALES simulations of linearly forced homogeneous turbulence[29] with progressively increasing Reynolds number are performed. For the details on linear forcing used in this work as well as description of governing equations solved using AWCM we refer to Ref. 23. All CVS and SCALES simulations are performed in the computational domain of $[0, 2\pi]^3$ on an adaptive grid with the base grid size of $\mathbf{M} = [m_x, m_y, m_z] = [8, 8, 8]$, which is dyadically refined/coarsened as needed such that the effective spatial grid resolution would be $\mathbf{M}2^{j-1}$ at the j level of resolution where the coarsest (minimum) level of the resolution is 2 and the highest level of resolution is 6, 7, 8, 9. These correspond to adaptive grids with nonadaptive effective resolutions of 256^3, 512^3, 1024^3, and 2048^3 at Taylor micro-scale Reynolds number of $Re_\lambda \cong 70, 120, 190, 320$ based on viscosities of $\nu = 0.09, 0.035, 0.015, 0.006$. These choices of viscosities are based on maintaining the ratio of Kolmogorov length-scale and the smallest grid-spacing constant, i.e., $\frac{\eta}{\Delta_{\min}} = 2$, to ensure the adequate resolution for a well-resolved DNS (analogous to the spectral DNS). This implies that by doubling the effective resolution the viscosity should be decreased by a factor of $2^{4/3}$ ($\Delta_{\min} \sim \mathfrak{N}_{1D}{}^{-1}$, $\eta \sim \nu^{3/4}$, $\Delta_{\min} \sim \eta \Rightarrow \nu \sim \mathfrak{N}_{1D}{}^{-4/3}$), since in linearly forced homogeneous turbulence the ratio of turbulence dissipation and turbulent kinetic energy, $\frac{\varepsilon}{\kappa}$, is kept constant.

VI. RESULTS

The broad objective of the present paper is to understand better the scaling of the number of spatial modes as a function of Reynolds number and the fidelity of the model, i.e., to estimate the exponent α in the relation, $\mathfrak{N} \sim Re^\alpha$, where $\mathfrak{N}$ is the number of spatial computational degrees of freedom of the turbulence. In order to quantify the model fidelity, it is useful to define "turbulence resolution," the quantity that measures the level to which one would like to resolve the most energetic/dynamically-important structures of turbulence. Turbulence resolution can be quantified differently. One way to define turbulence resolution is to use a ratio of subgrid scale and total turbulent kinetic energies, i.e., $\frac{k_{\text{sgs}}}{k_{\text{res}}+k_{\text{sgs}}}$, where k_{res} is the resolved turbulent kinetic energy and k_{sgs} is the SGS kinetic energy. However, since the energy spectrum decays with the increase of wave numbers, the SGS kinetic energy characterization of turbulence resolution is not appropriate for high Reynolds number flows, simply because it is mostly based on large-scale contribution and is not very sensitive to the Reynolds number changes. The SGS dissipation characterization, on the other hand, is a more objective measure since changes in molecular viscosity (Reynolds number) shift the peak of the resolved dissipation and enstrophy spectra to higher wavenumbers. For that reason in this work the turbulence resolution is measured by the ratio of dissipations rather than the ratio of kinetic energies of modeled and resolved structures. The local fraction of SGS dissipation (FSGSD, $\mathcal{F}$) is defined as $\frac{\Pi}{\varepsilon_{\text{res}}+\Pi}$, where $\varepsilon_{\text{res}} = 2\nu \widetilde{S_{ij}}^{\epsilon} \widetilde{S_{ij}}^{\epsilon}$ is the resolved viscous dissipation and $\Pi = -\tau_{ij}^* \widetilde{S_{ij}}^{\epsilon}$ is the local SGS dissipation.

In the light of this broad objective, we first perform the CVS and SCALES simulations with constant threshold levels $\epsilon = 0.2, 0.43$, respectively, which are set to based on earlier works on 256^3 turbulent simulations.[11,30] The performed simulations demonstrate consistency with $K^{-5/3}$ for the energy-spectra in particular at larger Reynolds number, where the inertial range is more pronounced, Figure 1. The vorticity magnitude and the adaptive computational mesh for SCALES simulations are illustrated in Figure 2. It is evident that how sparse is the adaptive grid of SCALES while it is able to resolve the energy-containing structures with such low number of spatial modes. The fixed scale for all vorticity field volume-rendered images, shows the augmentation of vorticity magnitude while the Reynolds number increases. The number of active wavelets ($\mathfrak{N}$) and the time-average of the *fraction of volume-averaged SGS dissipation* (total FSGSD) are listed in Table I. Total FSGSD

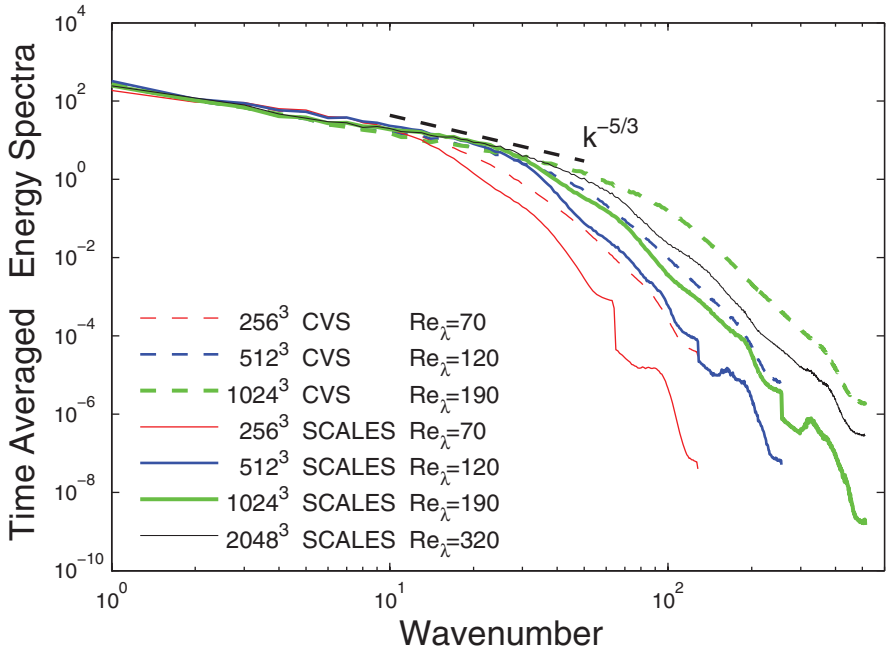

FIG. 1. Time-averaged energy spectra for CVS and SCALES at four different Reynolds numbers.

is defined as $\langle \mathcal{F} \rangle = \frac{\langle \Pi \rangle}{\langle \varepsilon_{\text{res}} \rangle + \langle \Pi \rangle}$, where $\langle \Pi \rangle = \langle -\tau_{ij}^{*} \overline{S}_{ij}^{\epsilon} \rangle$ and $\langle \varepsilon_{\text{res}} \rangle = 2\nu \langle \overline{S}_{ij}^{\epsilon} \overline{S}_{ij}^{\epsilon} \rangle$ are, respectively, the volume-averaged SGS and resolved viscous dissipations.

Figure 3 illustrates the percentage of active wavelets, which is $\mathfrak{D}$ divided by the corresponding nonadaptive effective resolution, $\mathfrak{D}_{\max}$. It is evident that the percentage of active spatial modes even decreases as Reynolds number increases; the compression ratio increases with the increase of Re_λ, which makes SCALES even more appealing for high Reynolds number flows. The computational complexity can be seen from the Re_λ scaling presented in Figure 4, which includes the DNS scaling as well. This study demonstrates that the spatial modes for CVS and SCALES scale slower than Re_λ^3

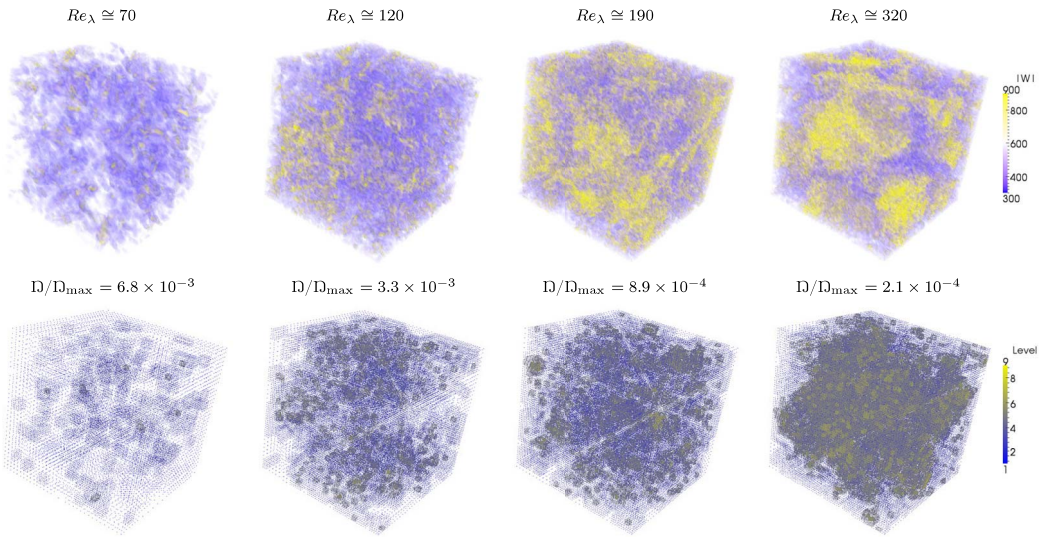

FIG. 2. Vorticity magnitude and the adaptive computational mesh for SCALES of linearly forced homogeneous turbulence on effective non-adaptive resolutions of 256^3, 512^3, 1024^3, 2048^3 at $Re_\lambda \cong 70, 120, 190, 320$.

TABLE I. Reference parameters.

Method	Re_λ	Resolution ($\mathfrak{D}_{max}$)	$\overline{\langle\mathcal{F}\rangle}$	$\mathfrak{D}$
CVS	70	256^3	...	1 100 000
CVS	120	512^3	...	5 000 000
CVS	190	1024^3	...	20 000 000
CVS	320	2048^3	...	90 000 000
SCALES	70	256^3	0.323178	115 000
SCALES	120	512^3	0.475869	437 000
SCALES	190	1024^3	0.594733	1 000 000
SCALES	320	2048^3	0.745060	1 850 000

and $Re_\lambda^{2.75}$, respectively, which compared with DNS scaling of $Re_\lambda^{9/2}$ implies considerably smaller exponents.

It is important to emphasize that both in CVS and SCALES, the scaling deviates from the constant slope as Reynolds increases. In SCALES, the main reason for this deviation is the increase of $\mathcal{F}$, reported in Figure 5. This implies that as Re_λ increases, the fidelity of the simulations decreases and the flow is relatively less resolved since the threshold-level was kept constant. The choice of $\epsilon = 0.43$ was based on optimum threshold for 256^3 simulation that is the maximum threshold at which SCALES matches the $\text{CVS}_{\epsilon_{opt}}$ spectra up to inertial range.[11] Therefore, using the same threshold for larger Re_λ implies the constant relative level of the resolution of the velocity field and consequently kinetic energy. In other words, the percentage of resolved kinetic energy is kept constant by using the same threshold value. As indicated at the beginning of this section, the kinetic energy characterization of turbulence resolution is not well suited for high Reynolds number flows, because the kinetic energy classification is mainly based on the large-scale contribution and is not sensitive to the Reynolds number variations. This implies that the complexity curves for both CVS and SCALES with constant thresholding eventually flatten out as Reynolds number increases.

It must be noted that the performed CVS with constant threshold value $\epsilon = 0.2$ on resolutions larger than 256^3 indeed is not the true CVS, mainly because it corresponds to the optimal threshold

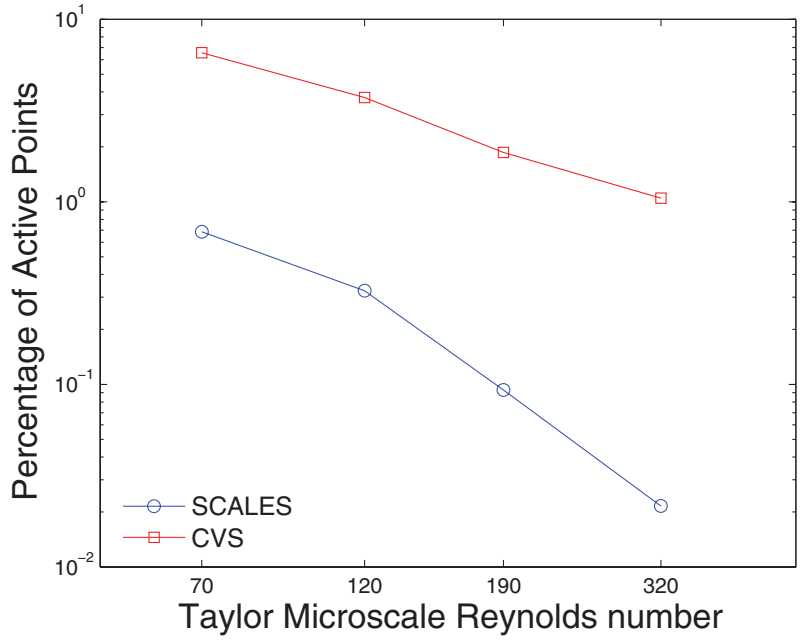

FIG. 3. Percentage of active wavelets, $\mathfrak{D}/\mathfrak{D}_{max}$, for CVS and SCALES with constant-threshold.

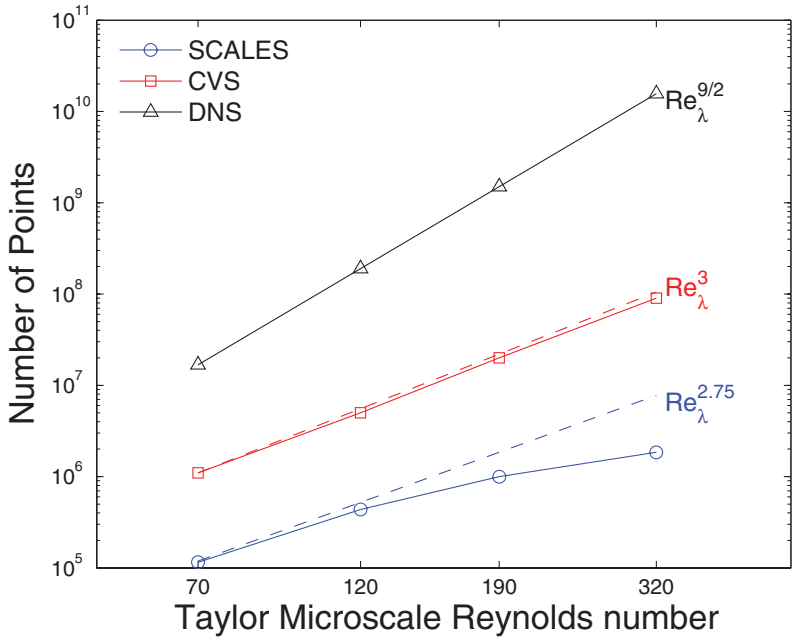

FIG. 4. Reynolds number scaling of CVS and SCALES with constant-threshold.

value for 256^3 case reported by Goldstein and Vasilyev[11] and Goldstein *et al.*[30] As explained before, the true CVS uses an optimal threshold to ensure that the unresolved field is the Gaussian white-noise and as a result its effect on the resolved field can be ignored. The use of larger threshold value results in additional mode truncation that removes the energy from the resolved field and, thus, acts as dissipative mechanism. This dissipation is responsible for slowing down of the scaling curve. Since the current study is based on velocity-pressure formulation of CVS, in order to find optimal

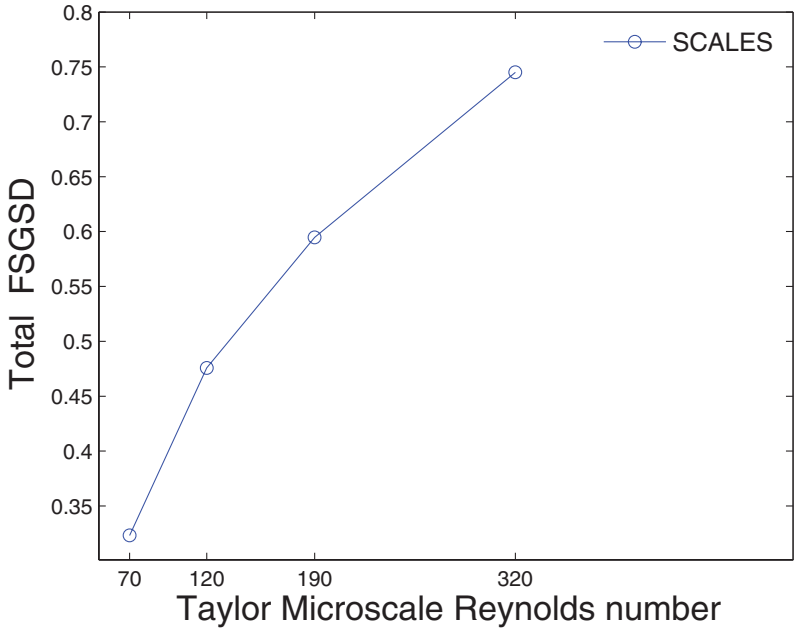

FIG. 5. Time-average of "fraction of volume-averaged SGS dissipation," $\overline{\langle \mathcal{F} \rangle} = \overline{\left(\frac{\langle \Pi \rangle}{\langle \varepsilon_{\text{res}} \rangle + \langle \Pi \rangle} \right)}$, for constant-threshold SCALES.

threshold value for CVS, one would need to conduct similar numerical experiments as in Goldstein and Vasilyev,[11] therefore, performing true CVS based on the ideal/optimal threshold is not practical for large Reynolds number turbulent flows.

When studying the Reynolds number scaling, it is important to maintain the fidelity of the simulations as Reynolds number changes. This can be achieved by keeping the fraction of the SGS dissipation, $\mathcal{F}$, constant, which would in turn ensure that the percentage of resolved dissipation or the turbulence resolution is approximately the same. Therefore, variable thresholding is utilized to maintain a constant level for $\mathcal{F}$. Both time varying[31] and spatially variable thresholding[15,32] approaches are used to maintain $\mathcal{F}$ for all Re_λ at the average value of $\mathcal{F}$ corresponding to the $Re_\lambda = 70$, i.e., $\mathcal{G} = \overline{\langle \mathcal{F} \rangle}_{256^3 \text{ with } \epsilon=0.43} \cong 0.32$, where $\mathcal{G}$ stands for the desired goal value for $\mathcal{F}$. Time varying thresholding was used only for $Re_\lambda = 70, 120$ and spatially variable thresholding was utilized for $Re_\lambda = 70, 120, 190, 320$. The results of both time and spatial variable thresholding are consistent and reported in Figure 6. Contrary to constant thresholding SCALES where the complexity slope was reducing, SCALES with this variable thresholding results in approximately constant slope. Comparison of percentage of number of active wavelets using spatially variable thresholding with constant thresholding as well as CVS is illustrated in Figure 7. It is important to discuss the fundamental difference between complexity studies of constant turbulence resolution SCALES and marginally resolved LES, discussed earlier. If the objective is only to resolve the turbulent kinetic energy, then the computational complexity of LES is insensitive to Reynolds number, while the requirement for LES to capture a certain fraction of turbulent dissipation/enstrophy results in a scaling exponent similar to DNS. Substantial decrease of the scaling exponent is a strong indication of the effective utilization of spatial intermittency by SCALES, contrasted to nearly DNS scaling of $Re_\lambda^{9/2}$ of marginally resolved LES.

In order to study the influence of the fidelity of simulation on the computational complexity of SCALES, a series of simulations of different turbulence resolution is conducted. The different fidelity is achieved by using spatially variable thresholding approach[15,32] with different goal values of $\mathcal{F}$, namely, $\mathcal{G} = 0.2, 0.25, 0.4, 0.5$ (Figure 8). It is observed that in the logarithmic scale the slope of Re_λ scaling of SCALES spatial modes at least up to 1024^3 remains approximately 4 while changing the level of turbulence resolution (Figure 9). In other words, the scaling exponent of constant-dissipation SCALES is nearly insensitive to the level of fidelity. It is interesting to note

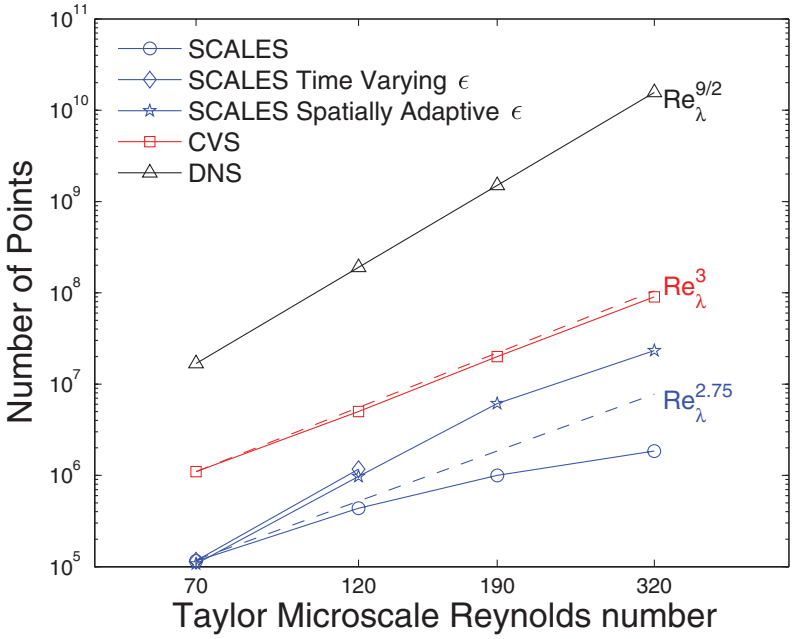

FIG. 6. Reynolds number scaling of constant-threshold CVS, constant-threshold SCALES, as well as both time and spatially adaptive ϵ SCALES.

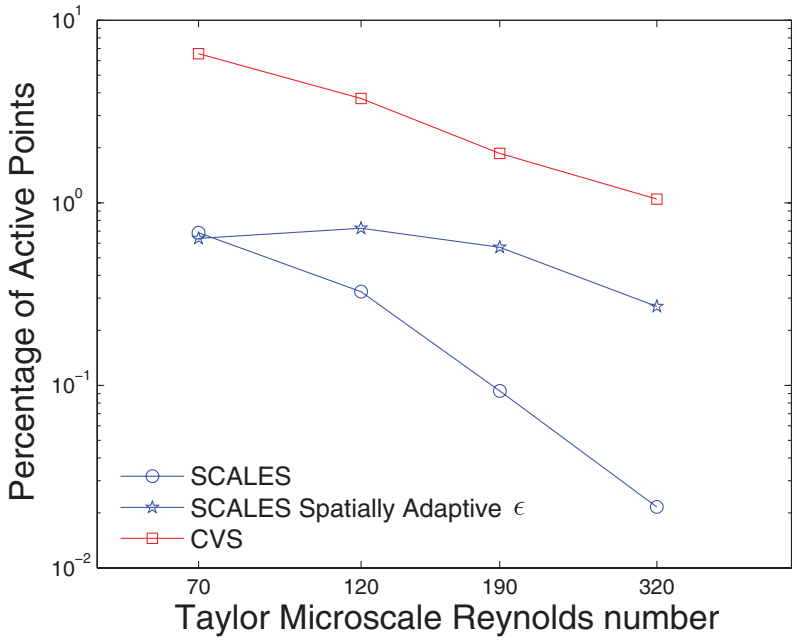

FIG. 7. Percentage of active wavelets, $\mathfrak{D}/\mathfrak{D}_{\max}$, for constant-threshold CVS, constant-threshold SCALES, and spatially adaptive ϵ SCALES.

that this scaling exponent is almost identical to the one of the vorticity-based CVS[12] for the *a priori* study of spectral DNS data. The similarity of scaling exponents is related to the fact that in homogeneous turbulence local enstrophy and viscous dissipation are strongly correlated. The scaling exponent for constant-dissipation SCALES is higher than constant-threshold CVS and SCALES, but lower than DNS. The percentage of active spatial modes initially either increases slightly or remains approximately constant as Reynolds number increases though eventually reduces similar to the constant-thresholding case (Figure 10). Thus, it can be concluded that the compression ratio is increasing as Reynolds increases regardless of constant-kinetic-energy or constant-dissipation

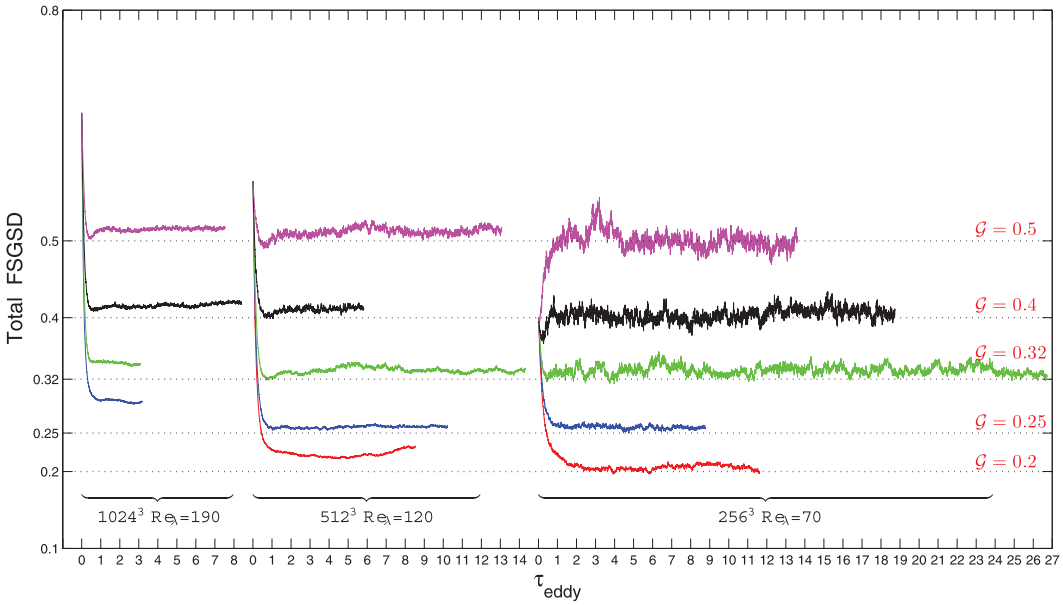

FIG. 8. Time-history of fraction of volume-averaged SGS dissipation, $\langle \mathcal{F} \rangle$, for constant-dissipation SCALES at various goal values.

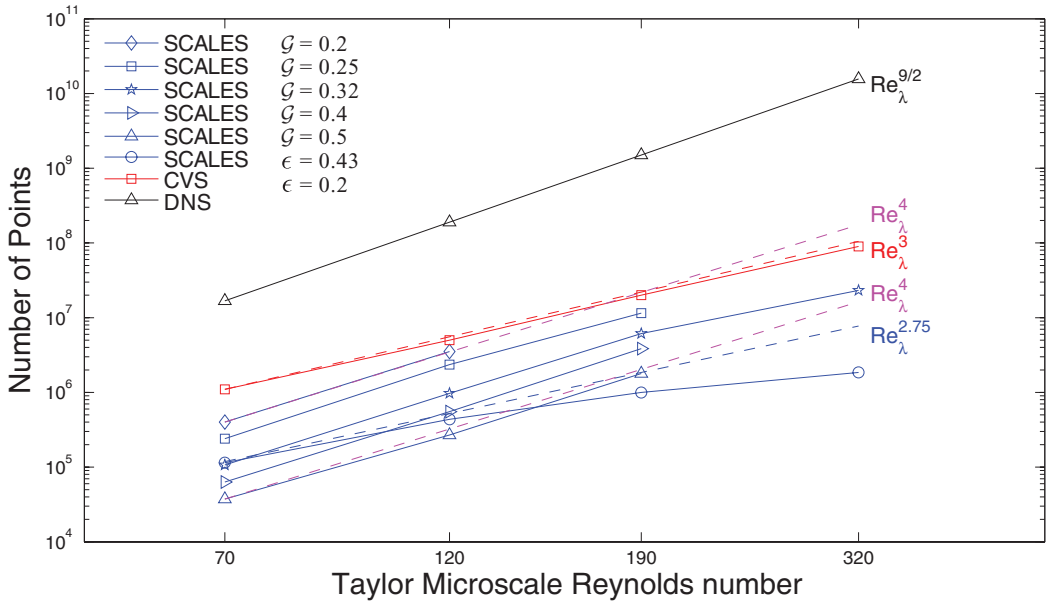

FIG. 9. Reynolds number scaling of constant-threshold CVS, constant-threshold SCALES, and constant-dissipation SCALES at various goal values.

simulation. Another important observation is that the dependence of the compression ratio on the turbulence resolution is quite strong and faster than $\mathcal{G}^{-2}$ for all Reynolds numbers studied (Figure 11).

Scrutinizing the SCALES results reveals that in the linear-scale instead of logarithmic-scale, the number of spatial modes for SCALES with constant threshold-level is growing linearly. This implies that the number of flow structures at a constant percentage of resolved kinetic energy is linearly increasing as Reynolds numbers grows (Figure 12).

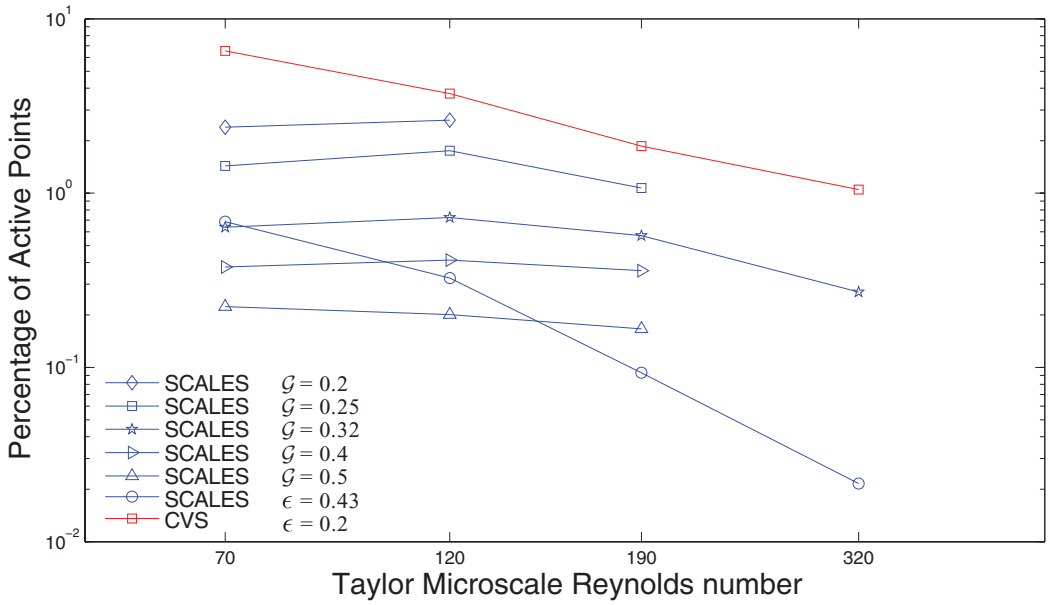

FIG. 10. Percentage of active wavelets, $\mathfrak{D}/\mathfrak{D}_{\max}$, for constant-threshold CVS, constant-threshold SCALES, and constant-dissipation SCALES at various goal values.

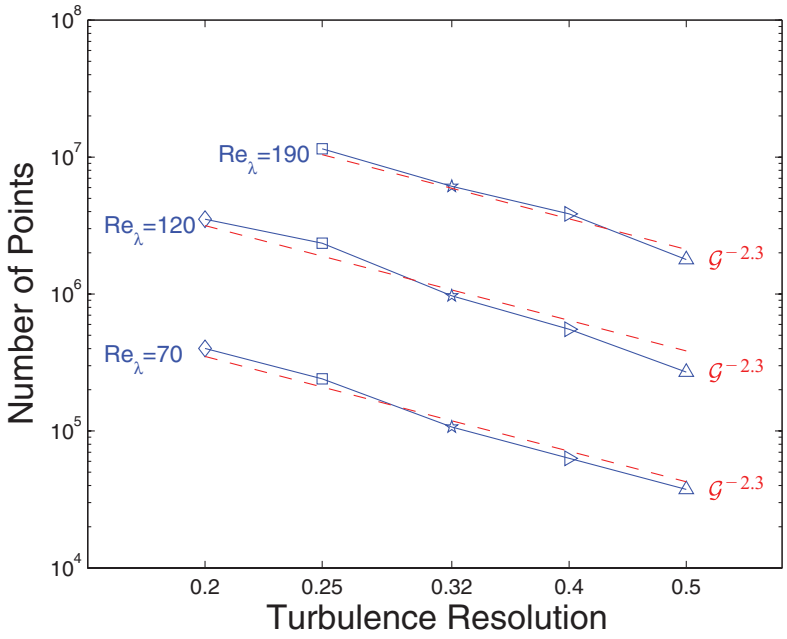

FIG. 11. Turbulence resolution scaling of constant-dissipation SCALES at different Reynolds number.

Comparison of time-averaged energy spectra of CVS, SCALES with constant threshold, and constant-dissipation SCALES with different goal values for both 256^3 and 512^3 resolutions are provided in Figure 13. Improvements in spectra by decreasing $\mathcal{G}$ for any Reynolds number clearly illustrate that the defined turbulence resolution $\mathcal{F}$ is a physically meaningful measure. It is worth clarifying that for both Reynolds numbers, proximity of spectra of both constant-threshold SCALES

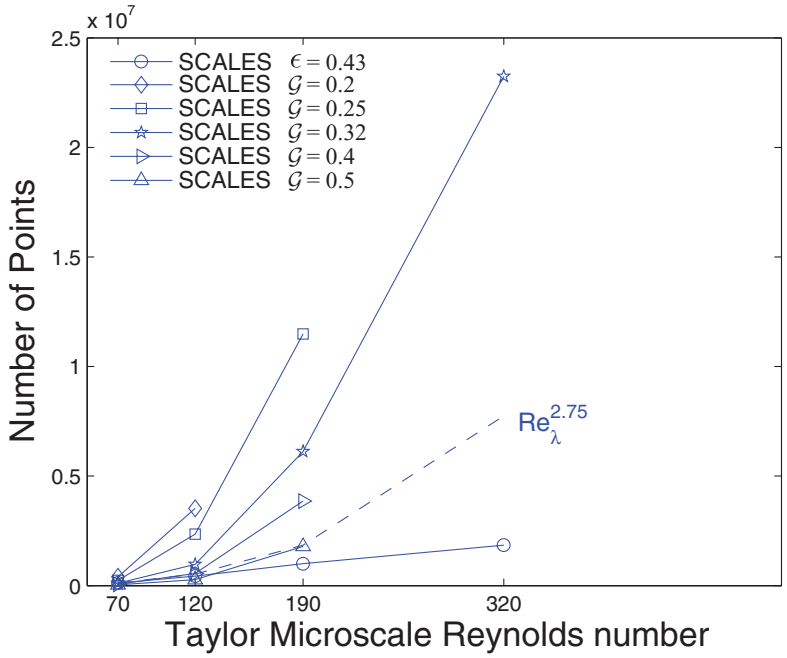

FIG. 12. Reynolds number scaling of constant-threshold CVS, constant-threshold SCALES, and constant-dissipation SCALES at various goal values in linear scale.

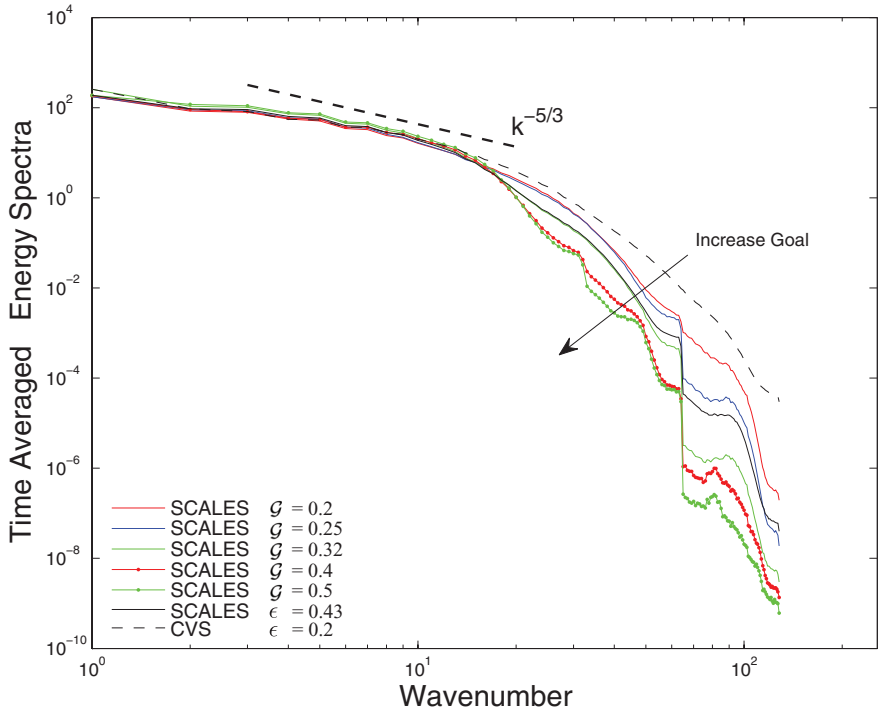

(a) $Re_\lambda = 70, 256^3$

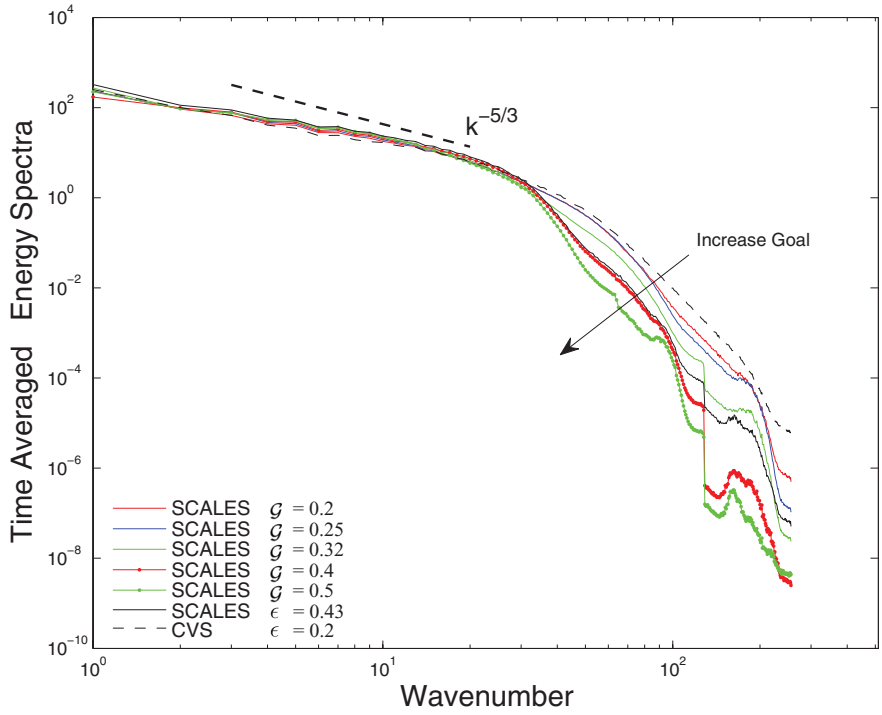

(b) $Re_\lambda = 120, 512^3$

FIG. 13. Time-averaged energy spectra of constant-threshold CVS, constant-threshold SCALES, and constant-dissipation SCALES at various goal values for two different Reynolds number.

with $\epsilon = 0.43$, and constant-dissipation SCALES with $\mathcal{G} = 0.32$ is natural and expected since $\mathcal{G} = 0.32$ is indeed approximately equal to $\overline{\langle \mathcal{F} \rangle}_{256^3 \text{ with } \epsilon=0.43}$.

The fractal dimension and consequently the intermittency of the active regions of the flow can be estimated analogously to the analysis of Paladin and Vulpiani[33] and Kevlahan *et al.*[3] who utilized the β-model of Frisch *et al.*,[34] which shows that the spatial degrees-of-freedom of an intermittent turbulent flow should scale like $Re^{3D_F/(D_F+1)}$, where $D_F \leq 3$ is the fractal dimension of the active part of the turbulent flow. It is observed that the fractal dimensions for constant-threshold CVS and SCALES are $D_{F_{\text{CVS}}} \lesssim 1$ and $D_{F_{\text{SCALES}}} \lesssim \frac{11}{13}$, respectively, while fractal dimension of constant-dissipation SCALES is of the order of $D_{F_{\text{cd SCALES}}} \lesssim 2$. The most intriguing part about these findings is very low, close to unity, fractal dimension of the energy containing structures and fractal dimension close to two for enstrophy containing structures.

VII. CONCLUSION

While DNS of the real flow applications will most definitely remain impossible for our generations, and the large/small structures decomposition in LES has its own challenges in particular for wall-bounded flows, the coherent/incoherent and more/less-energetic structures decomposition in CVS and SCALES, respectively, are very promising tools for numerical simulations of highly intermittent both homogeneous and inhomogeneous turbulent flows at high Reynolds numbers. This investigation is the first attempt to prove this argument by demonstrating very promising slope for Reynolds number scaling of SCALES.

This work is the first effort to present *dynamic* complexity study of coherent vortex simulation and adaptive wavelet-based large eddy simulation to quantitatively justify the power of both CVS and SCALES. The performed Reynolds number scaling study shows that in SCALES even with preserving a constant level of turbulence resolution while increasing the Reynolds number, the required number of DOFs is still smaller than CVS and DNS for relatively large Reynolds numbers. This computational complexity study utilizes extensively the capability of a recently developed spatially variable thresholding technique in order to accomplish the scaling based on constant level of SGS dissipation to the total dissipation, i.e., a constant level of turbulence resolution. The scaling statistics presented in this work proves that the developed model can resolve more flow-physics phenomena yet with considerably smaller number of spatial modes compared with marginally resolved LES. It is demonstrated that depending on the level of details the flow physics is captured, the same model and the same numerical method result in different Reynolds number scaling.

This computational complexity study has also drawn two insightful physical conclusions: the number of flow structures at a constant percentage of resolved kinetic energy – i.e., number of fixed-energy containing structures (energy containing structures at a fixed level of kinetic energy) – scales linearly with Reynolds number. Furthermore, the fractal dimension – which provides a qualitative measure of how intermittent the turbulent flow is – in both constant-threshold SCALES and CVS is close to unity, while for constant-dissipation SCALES it is close to two.

ACKNOWLEDGMENTS

This work was supported by NSF under Grant Nos. CBET-0756046 and CBET-1236505. This support is gratefully acknowledged. Authors are also thankful for the computing time on the Janus supercomputer, which is supported by the National Science Foundation (Award No. CNS-0821794) and the University of Colorado Boulder. The Janus supercomputer is a joint effort of the University of Colorado Boulder, the University of Colorado Denver, and the National Center for Atmospheric Research.

[1] D. Fox and D. Lilly, "Numerical simulation of turbulent flows," Rev. Geophys. Space Phys. **10**, 51–72, doi:10.1029/RG010i001p00051 (1972).
[2] P. Moin and K. Mahesh, "Direct numerical simulation: A tool in turbulence research," Annu. Rev. Fluid Mech. **30**, 539–578 (1998).
[3] N. K.-R. Kevlahan, J. Alam, and O. V. Vasilyev, "Scaling of space-time modes with Reynolds number in two-dimensional turbulence," J. Fluid Mech. **570**, 217–226 (2007).

[4] C. Foias and G. Prodi, "Sur le comportement global des solution non stationnaires des quations de Navier-Stokes en dimension deux," Rend. Sem. Math. Univ. Padova **39**, 1–34 (1967).
[5] G. P. Galdi, "Determining modes, nodes and volume elements for stationary solutions of the Navier-Stokes problem past a three-dimensional body," Arch. Rat. Mech. Anal. **180**, 97–126 (2006).
[6] V. Yakhot and K. R. Sreenivasan, "Anomalous scaling of structure functions and dynamic constraints on turbulence simulations," J. Stat. Phys. **121**, 823–841 (2005).
[7] P. Moin, "Advances in large eddy simulation methodology of complex flows," Int. J. Heat Fluid Flow **23**, 710–720 (2002).
[8] U. Piomelli and E. Balaras, "Wall-layer models for large-eddy simulations," Annu. Rev. Fluid Mech. **34**, 349–374 (2002).
[9] K. Schneider and O. V. Vasilyev, "Wavelet methods in computational fluid dynamics," Annu. Rev. Fluid Mech. **42**, 473–503 (2010).
[10] M. Farge, K. Schneider, and N. K.-R. Kevlahan, "Non-Gaussianity and coherent vortex simulation for two-dimensional turbulence using an adaptive orthogonal wavelet basis," Phys. Fluids **11**, 2187–2201 (1999).
[11] D. E. Goldstein and O. V. Vasilyev, "Stochastic coherent adaptive large eddy simulation method," Phys. Fluids **16**, 2497–2513 (2004).
[12] N. Okamoto, K. Yoshimatsu, K. Schneider, M. Farge, and Y. Kaneda, "Coherent vortices in high resolution direct numerical simulation of homogeneous isotropic turbulence: A wavelet viewpoint," Phys. Fluids **19**, 115109 (2007).
[13] N. Okamoto, K. Yoshimatsu, K. Schneider, M. Farge, and Y. Kaneda, "Coherent vorticity simulation of three-dimensional forced homogeneous isotropic turbulence," Multiscale Model. Simul. **9**, 1144–1161 (2011).
[14] G. De Stefano and O. V. Vasilyev, "Perfect modeling framework for dynamic SGS model testing in large eddy simulation," Theor. Comput. Fluid Dyn. **18**, 27–41 (2004).
[15] A. Nejadmalayeri, "Hierarchical multiscale adaptive variable fidelity wavelet-based turbulence modeling with Lagrangian spatially variable thresholding," Ph.D. thesis (University of Colorado Boulder, Boulder, CO, 2012).
[16] I. Daubechies, *Ten Lectures on Wavelets*, CBMS-NSF Series in Applied Mathematics Vol. 61 (SIAM, 1992).
[17] O. V. Vasilyev and C. Bowman, "Second generation wavelet collocation method for the solution of partial differential equations," J. Comput. Phys. **165**, 660–693 (2000).
[18] O. V. Vasilyev, "Solving multi-dimensional evolution problems with localized structures using second generation wavelets," Int. J. Comput. Fluid Dyn. **17**, 151–168 (2003).
[19] O. V. Vasilyev and N. K.-R. Kevlahan, "An adaptive multilevel wavelet collocation method for elliptic problems," J. Comput. Phys. **206**, 412–431 (2005).
[20] N. K. R. Kevlahan and O. V. Vasilyev, "An adaptive wavelet collocation method for fluid-structure interaction at high Reynolds numbers," SIAM J. Sci. Comput. **26**, 1894–1915 (2005).
[21] W. Sweldens, "The lifting scheme: A construction of second generation wavelets," SIAM J. Math. Anal. **29**, 511–546 (1998).
[22] J. D. Regele and O. V. Vasilyev, "An adaptive wavelet-collocation method for shock computations," Int. J. Comput. Fluid Dyn. **23**, 503–518 (2009).
[23] G. De Stefano and O. V. Vasilyev, "Stochastic coherent adaptive large eddy simulation of forced isotropic turbulence," J. Fluid Mech. **646**, 453–470 (2010).
[24] G. De Stefano and O. V. Vasilyev, "Wavelet-based adaptive large-eddy simulation with explicit filtering," J. Comput. Phys. **238**, 240–254 (2013).
[25] S. J. Reckinger, D. Livescu, and O. V. Vasilyev, "Adaptive wavelet collocation method simulations of Rayleigh-Taylor instability," Phys. Scr. **T142**, 014064 (2010).
[26] S. M. Reckinger, O. V. Vasilyev, and B. Fox-Kemper, "Adaptive volume penalization for ocean modeling," Ocean Dyn. **62**, 1201–1215 (2012).
[27] J. D. Regele, D. R. Kassoy, and O. V. Vasilyev, "Effects of high activation energies on acoustic timescale detonation initiation," Combust. Theory Modell. **16**, 650–678 (2012).
[28] J. Fröhlich and K. Schneider, "Numerical simulation of decaying turbulence in an adaptive wavelet basis," Appl. Comput. Harmon. Anal. **3**, 393–397 (1996).
[29] C. Rosales and C. Meneveau, "Linear forcing in numerical simulations of isotropic turbulence: Physical space implementations and convergence properties," Phys. Fluids **17**, 095106 (2005).
[30] D. E. Goldstein, O. V. Vasilyev, and N. K.-R. Kevlahan, "CVS and SCALES simulation of 3D isotropic turbulence," J. Turbul. **6**, N37 (2005).
[31] G. De Stefano and O. V. Vasilyev, "A fully adaptive wavelet-based approach to homogeneous turbulence simulation," J. Fluid Mech. **695**, 149–172 (2012).
[32] A. Nejadmalayeri, O. V. Vasilyev, A. Vezolainen, and G. De Stefano, "Spatially variable thresholding for stochastic coherent adaptive LES," in *Proceedings of Direct and Large-Eddy Simulation Workshop 8: Eindhoven University of Technology, the Netherlands, July 7–9, 2010*, edited by H. Kuerten, B. Geurts, V. Armenio, and J. Fröhlich (Springer, 2011), pp. 95–100.
[33] G. Paladin and A. Vulpiani, "Degrees of freedom of turbulence," Phys. Rev. A **35**, 1971–1973 (1987).
[34] U. Frisch, P.-L. Sulem, and M. Nelkin, "A simple dynamical model of intermittent fully developed turbulence," J. Fluid Mech. **87**, 719–736 (1978).